Mechanical properties and crown adaptation accuracy of additively manufactured zirconia restorations

Sae-Eun Oh

The Graduate School

Yonsei University

Department of Dentistry

Mechanical properties and crown adaptation accuracy of additively manufactured zirconia restorations

Directed by Professor YoungBum Park

A Dissertation

Submitted to the Department of Dentistry

and the Graduate School of Yonsei University

in partial fulfillment of the

requirements for the degree of

Doctor of Philosophy in Dental Science

Sae-Eun Oh

June 2024

This certifies that the Doctoral Dissertation
of Sae-Eun Oh is approved.

_____
Thesis Supervisor: YoungBum Park

_____
June-Sung Shim

_____
Jee-Hwan Kim

_____
Ji-Man Park

_____
Hyung-Jun Kim

The Graduate School
Yonsei University
June 2024

감사의 글

북경대학 치대를 졸업하고 연세대학교 치과대학에서 보낸 시간들은 저에게 매우 뜻 깊은 시간이었습니다. 많은 분들의 지지와 도움으로 학부, 인턴, 레지던트 그리고 대학원 과정을 무사히 잘 마칠 수 있게 되었습니다.

먼저 저를 여기까지 이끌어 주시고 도움을 주신 박영범 교수님께 진심으로 감사드립니다. 치과의사로서, 학자로서의 귀감을 보여주셨을 뿐만 아니라 인생의 길잡이가 되어주심에 깊은 존경을 표합니다. 또한 학부 때부터 지켜 봐주시고 지지해주신 심준성 교수님께 존경과 감사를 전합니다. 언제나 따뜻하게 맞아주시고 가르침을 베풀어주시는 김형준 교수님께도 깊은 감사를 드립니다. 학술적인 조언뿐만 아니라 치과의사로서 잊지 말아야 할 기본을 몸소 보여주시고 배우게 해주신 김지환 교수님께 깊은 감사를 드립니다. 바쁘신 중에 논문을 맡아주시고, 이 연구를 포기하지 않게 아낌없는 지원과 도움을 주신 박지만 교수님께 깊은 감사의 마음을 전합니다.

제가 하고 싶은 것은 무엇이든지 할 수 있게 지지해주시고 도와주시는 세상에서 가장 사랑하는 오태환 아버지, 문옥순 어머니 정말 감사합니다. 본인도 박사 과정 중임에도 항상 언니를 먼저 챙겨주는 우리 세란이, 든든하게 큰누나 몫까지 마음 써주는 우리 막내 세윤이에게 고마움과 사랑을 전합니다.

마지막으로 교수님들께서 베풀어 주신 은혜와 가르침 마음속 깊이 새기고, 저 또한 베풀 수 있는 사람이 되도록 노력하겠습니다. 박영범 교수님, 심준성 교수님, 김형준 교수님, 김지환 교수님 그리고 박지만 교수님, 저의 스승님이 되어 주셔서 정말 감사합니다.

2024 년 6 월

오 세 은

TABLE OF CONTENTS

LIST OF FIGURES

LIST OF TABLES

ABSTRACT

Mechanical properties and crown adaptation accuracy of additively manufactured zirconia restorations

Sae-Eun Oh

Department of Dentistry

The Graduate School, Yonsei University

(Directed by Professor YoungBum Park, D.D.S., M.S., PhD.)

We evaluated the mechanical properties of zirconia restorations produced via additive manufacturing (AM) and the clinical applicability of zirconia crowns. Zirconia disks, bars, and crowns were manufactured via subtractive (CNC group) and additive manufacturing (AM group) techniques. Disk-shaped specimens in each group were autoclaved at 134 °C and 216 kPa for 5, 10, and 24 h. The phases of the specimens were analyzed using an X-ray diffractometer. The flexural strengths were measured via biaxial flexural tests. The morphologies were examined using a scanning electron microscope. The correlation between the m-phase fraction and biaxial flexural strength by autoclave time in each group was analyzed via

linear mixed model and Pearson's correlation analysis. For each group, crown specimens were used to assess the marginal and internal gaps using the replica technique. Buccolingual and mesiodistal cross-sections were measured, and non-inferiority trials and repeated measures one-way ANOVA were performed. Linear mixed model analysis indicated that for both groups, with an increase in the autoclave time, the flexural strength decreased, whereas the m-phase fraction increased. Pearson's correlation analysis revealed no correlation between the m-phase fraction and flexural strength for either group. The non-inferiority trials on instrumented sections (buccal, lingual, mesial, and distal) indicated that the gap of the AM group was inferior to that of the CNC group in all sections, except for the distal occlusal section (lower limit confidence interval < −33). A repeated measures one-way ANOVA was conducted on instrumented sections (buccal, lingual, mesial, and distal), revealing that the marginal and internal gaps of AM-produced zirconia crowns was less accurate than CNC-produced zirconia crowns. These findings suggest that additively produced zirconia restorations have mechanical properties comparable to those of conventionally produced ceramics and may be suitable for clinical applications.

Keywords: 3D-printed zirconia; additive manufacturing; flexural strength; low-temperature degradation; replica technique

Mechanical properties and crown adaptation accuracy of additively manufactured zirconia restorations

Sae-Eun Oh

Department of Dentistry
The Graduate School, Yonsei University

(Directed by Professor YoungBum Park, D.D.S., M.S., PhD.)

I. Introduction

Zirconia (ZrO_2) is a ceramic material with a multitude of beneficial characteristics. These include high resilience, high flexural strength, high wear resistance, excellent insulating properties, the capacity to function as a thermally insulative material at ambient temperature, and electrical conductivity at elevated temperatures. Zirconia ceramics have a diverse range of applications in various fields. In the electronics industry, zirconia ceramics are utilized as the primary materials for components such as insulators, substrates, and capacitors. Moreover, zirconia ceramics are utilized in a multitude of machining applications, including the fabrication of cutting tools and wear-resistant components. Furthermore, zirconia ceramics are utilized in the aerospace industry due to their capacity

to withstand severe temperatures and mechanical stresses. In addition, zirconia ceramics are employed as electrolyte materials for solid oxide fuel cells in fuel cell technology. Zirconia ceramics are utilized in the production of ceramic bearings and valves, as well as in thermal barrier coatings in the aviation industry. Moreover, zirconia has been investigated as a potential replacement for titanium in the medical field due to its exceptional wear resistance and biocompatibility. In 1969, the first attempt was made to use zirconia in place of titanium or alumina in hip replacements in the orthopedic field (Willmann et al., 1996). Currently, the fourth generation of zirconia ceramics, which contains 17% zirconia and is added to alumina, is employed in ceramic-ceramic articular surface hip replacements. In dentistry, zirconia is known for its superior physical strength, biocompatibility, slight transparency, and masking ability compared with conventional ceramics, which led Garvie to call it “ceramic steel” in 1975 (Garvie et al., 1989). Zirconia has a unique property: when stimulated from the outside, it creates compressive stress within itself, which prevents crack propagation. This is a breakthrough property that compensates for brittleness, which is the most vulnerable property of ceramics (Christel et al., 2008; Kelly et al. 2008). Zirconia is a polymorphic material with three allotropes: a monoclinic phase, which is stable up to 1170 °C, a tetragonal phase up to 2370 °C, and a cubic phase from 2370 °C to its melting point at 2680 °C. When a transformation from the tetragonal phase (t) to the monoclinic phase (m) occurs, which can be induced by externally applied stresses such as those induced by trimming, impact, or fracture, a volume expansion

of 3%–5% occurs, which induces the development of internal stresses against crack initiation and ultimately increases the resistance of the material to crack propagation. This phase transformation of zirconia allows the toughening method to overcome to a certain extent the brittleness, which is the main drawback of ceramics, and has led to its application in many areas of dental restoration, such as crowns, implant abutments, inlays, and onlays. With the addition of oxides (CaO, MgO, CeO_2, and Y_2O_3) that stabilize the phase transformation of zirconia, zirconia remains undeformed and metastable below the temperature at which it transforms from the tetragonal phase (t) to the monoclinic phase (m). Currently, zirconia-yttria (ZrO_2-Y_2O_3) materials, which are known as yttria-stabilized tetragonal zirconia polycrystals (Y-TZP), are widely used. The mechanical properties of 3 mol% Y-TZP (3Y-TZP) are superior to those of all other available dental ceramics, with a flexural strength in the range of 800–1000 MPa (Denry et al. 2008).

In the 1980s, attempts were made to produce dental prostheses using computer-aided design/computer-aided manufacturing (CAD/CAM) technology, and the rapid evolution of CAD/CAM technology has significantly impacted all areas of dentistry—particularly prosthodontics and restorative dentistry (Rekow, 1987; Leinfelder et al. 1989; Rekow ED, 1991; van der Zel, 1993). Dental CAD/CAM methods can be categorized as subtractive manufacturing (SM) and additive manufacturing (AM). SM involves computer numerical control (CNC) of pre-sintered or sintered zirconia blocks to achieve a definitive shape and volume of the restoration (Torabi et al. 2015). Compared with traditional dental

laboratory technology, CAD/CAM systems are now the gold standard for creating ceramic fixed prostheses because of their ability to incorporate new materials, reduced labor, cost-effectiveness, and quality control (Alghazzawi, 2016). In most dental applications, CAD/CAM systems utilize the cutting method of machining, which involves milling a block of solid ceramics using a milling bur to achieve the desired shape. However, this method has disadvantages, such as difficulty in producing complex models, significant material waste, and a short consumable life (Dawood et al. 2015; Abduo et al. 2014). To overcome these disadvantages, a method for processing ceramic materials by combining additive manufacturing with three-dimensional (3D) printing has been proposed. The transition from this subtractive manufacturing to additive manufacturing using 3D printing is gaining momentum with the advent of the fourth industrial revolution, which represents a merger of intelligent information technologies based on the third industrial revolution, which was represented by computers and the Internet, with information and communication technologies. The benefits of 3D printing in dentistry include the ability to create objects with any desired geometry, even if it is highly complex, and to customize them to fit the individual needs of patients. Various AM techniques have been used to manufacture zirconia objects, including vat photopolymerization (stereolithography and direct light processing), selective laser sintering, selective laser melting, inkjet printing, fused deposition modeling, direct energy deposition, sheet lamination, and binder jetting. Vat photopolymerization technologies are defined as “additive manufacturing processes in

which liquid photopolymer in a vat is selectively cured by light-activated polymerization." This includes techniques such as stereolithography (SLA) and digital light processing (DLP) (Deckers J, 2014). SLA is an alternative vat polymerization method that involves the laser beam raster scanning of the surface within a tank with a photosensitive liquid—generally a photopolymerizable resin (Taormina et al. 2018). In contrast to SLA, in which the laser beam moves across the layer surface, causing localized polymerization of the photosensitive resin in the illuminated field, DLP simultaneously cures the entire material portion in the x/y space via a single projection of the entire layer through the light projector (Stansbury et al. 2015). Among the various AM technologies, SLA is preferred for dental applications because it provides the highest accuracy and resolution and a flawless surface finish (Della et al. 2021). Compared with SLA technology, DLP technology has advantages such as the ability to produce large models and faster printing; however, the relatively high cost of printers makes its widespread use difficult. With the advancement of ceramic 3D-printing technology, companies have been able to produce additively manufactured zirconia restorations. However, these restorations are still in their infancy and not routinely used in clinical practice. This is because there have been few studies on the properties and clinical applicability of 3D-printed additive zirconia ceramics, whereas the properties and clinical applicability of machined zirconia ceramics are well documented in the literature.

The objective of the present study was to compare the mechanical properties and crown accuracy of zirconia restorations produced using the AM and CNC technologies.

The null hypotheses were as follows: (1) the mechanical properties (m-phase fraction, flexural strength by autoclave time) of AM-produced 3Y-TZP are comparable to those of CNC-produced 3Y-TZP restorations, and (2) the marginal and internal gaps of AM-produced 3Y-TZP are comparable to those of CNC-produced 3Y-TZP crowns.

II. Materials and Methods

1. Sample preparation

The zirconia specimens were produced using two different manufacturing techniques: milling (CNC group) and additive manufacturing (AM group). The disks, crowns, and dies were designed using a Rhinoceros 3D modeling software (Rhinoceros 3D, Rhino, Robert McNeel, and Associates for Windows, Washington DC, USA). The dimensions of the disk- and bar-shaped specimens were as specified by the ISO/CD 6872 standard (10 × 1.2 ± 0.2 mm and 25 × 4 × 3 ± 0.2 mm) (Figure 1). All specimens had an A2 shade. The dimensions of all the disks and bars were confirmed to be accurate within 0.01 mm using digital calipers (ASB Digimatic Calipers, Mitutoyo Co., Kawasaki, Japan).

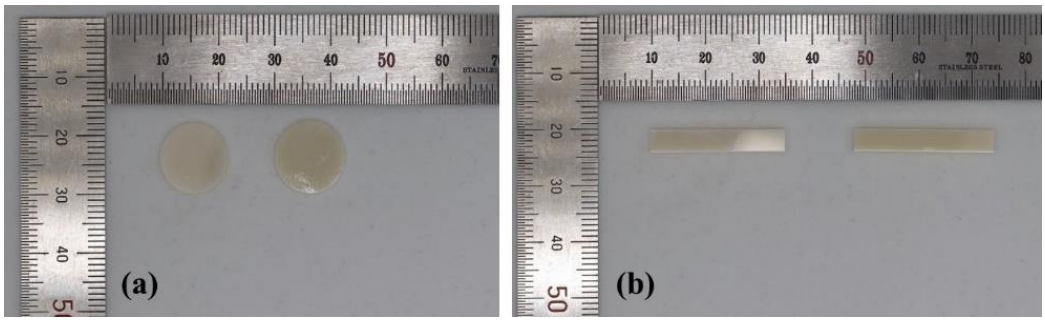

Figure 1. Zirconia specimens: (a) disk-shaped specimens (left, AM group; right, CNC group); (b) bar-shaped specimens (left, AM group; right, CNC group).

For this *in vitro* study, a machined standard stainless-steel master die with a height of 5.925 mm and width of 7.850 mm was prepared. The die had a 90° shoulder marginal finish line with a width of 0.4 mm and a convergence angle of 11° (5.5 for each axial wall). A marker was present on the buccal aspect of the model, as shown in Figures 2 and 3. The master die was produced using Spherical APA™ Ti-6Al-4V Powder (AP&C, Quebec, Canada) with a layer thickness (z-axis) of 30 μm by employing a 3D printer (Mlab 200 R, Concept Laser, Lichtenfels, Germany).

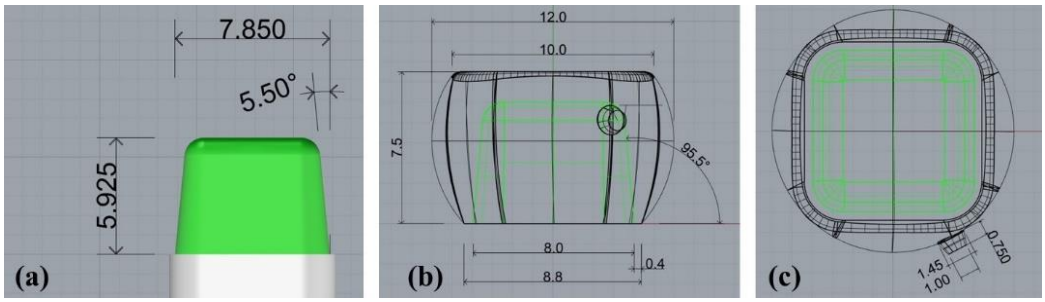

Figure 2. CAD designs: (a) master die design, (b) crown design (buccal view); (c) crown design (occlusal view).

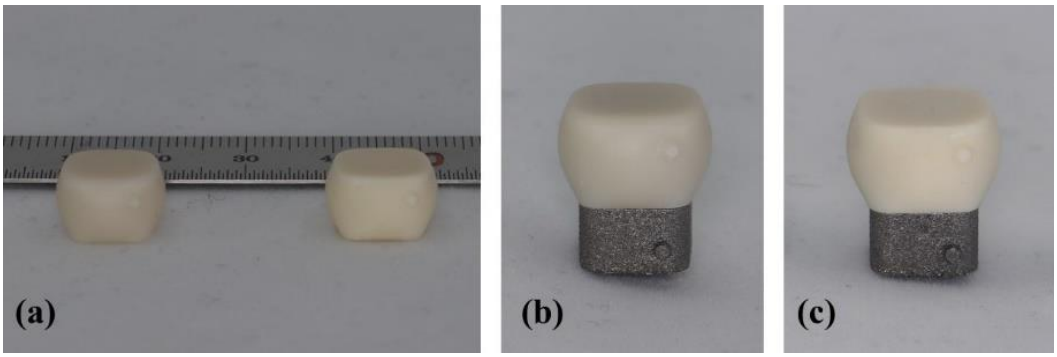

Figure 3. Zirconia crowns and master dies: (a) crown specimens (left, CNC group; right, AM group); (b) CNC-technology-fabricated zirconia crown was seated on the master die; (c) AM-technology-fabricated zirconia crown was seated on the master die.

After scanning the stainless-steel master die, we fabricated the crowns. They were designed to have a thickness of 0.4 mm, a cement space of 40 μm, and a buccal marker to aid in alignment during measurement (Figures 2 and 3). The design file was loaded into a 3D printer-specific slicer program (DentiqGuide; 3D Industrial Imaging Co, Ltd., Seoul, Korea) to generate printing instructions for the individual layers.

For the CNC group, 40 disks, 10 bars, and 10 crowns of milled 3 mol% Y_2O_3 tetragonal zirconia polycrystals (KATANA HT, Kurary Noritake Dental Inc., Miyoshi, Japan) with the same dimensions were fabricated using a five-axis milling machine (IDC MILL 5X, Amann Girrbach AG, Koblach, Austria). The process involved placing a pre-sintered zirconia block in the holder of the milling machine. Three different burr sizes (2.0, 1.0, and 0.5 mm) were used for the milling to achieve a detailed and smooth specimens surfaces. Following the milling, the green objects were sintered at 1500 °C to produce fully dense ceramic disks and crowns.

For the AM group, a standard tessellation language (STL) file was utilized to produce 40 disks, 10 bars, and 10 crowns using 3 mol% Y_2O_3 tetragonal zirconia paste (3DMAT500A2; Genoss Co.) with a 3D printer (Veltz-Cera90, Veltz 3D) and DLP printing technology. The layer thickness (z-axis) was set as 50 μm, and post-processing procedures were carried out according to the manufacturer's instructions. The fabrication of the AM zirconia samples was conducted by a researcher with expertise in this field. The specifics of this process are not disclosed due to patent and security regulations.

2. Microstructural observations

The microstructures were examined via field-emission scanning electron microscopy (FE-SEM; Merlin, Zeiss, Land Baden-Württemberg, Germany).

3. Zirconia phase quantification via X-ray diffraction

The zirconia phase fractions were quantified via X-ray diffraction (XRD) analysis for sintered and polished plate specimens (10×1.2 ± 0.2 mm). Scans were performed in the 2θ range of 25°–35° with a step size of 0.01° and 0.5 s/step intervals using an X-ray diffractometer (SmartLab, Rigaku).

The m-phase fraction (X_m) was calculated using the following equation:

$$X_m = [\, I_{M(111)} + I_{M(11\bar{1})} \,] \times 100 / [\, I_{M(111)} + I_{M(11\bar{1})} + I_{T(111)} \,],$$

where $I_{M(111)}$ represents the intensity of the peak (area under the 31.5° peak) that corresponds to the m-phase (111), $I_{M(11\bar{1})}$ represents the intensity of the peak (area under the 28.2° peak) that corresponds to the m-phase ($11\bar{1}$), and I_T represents the intensity of the peak that corresponds to the t-phase. Forty disk specimens from each group were measured, and the mean and standard deviation (SD) were calculated.

4. Low-temperature degradation

Autoclave treatment accelerates the low-temperature degradation (LTD) of zirconia ceramics. An LTD test was performed in accordance with the ISO 13356 standard. Autoclaving was performed at 134 °C and 216 kPa for 5, 10, and 24 h in an autoclave chamber (Hydrothermal Reactor, Kodam Co., Seoul, Korea) after annealing, grinding, and sandblasting the specimens.

5. Flexural strength

The flexural strengths of the CNC and AM groups were measured in accordance with ISO/CD 6872 using a universal testing machine (Instron Model 3366; Instron Corp.). The disc specimens were tested using a piston-on-three-ball apparatus (biaxial flexural strength (BFS) testing), and the bar specimens were tested using a three-point apparatus (3-point flexural strength testing). The specimens were subjected to a load applied at the center of the supporting point at a crosshead speed of 0.5 mm/min until they started to crack. The load (N) values at which the specimens cracked were recorded.

The BFS of each specimen was calculated using the following equation obtained from ISO Standard 6872 with the Poisson's ratio for the dental ceramic set as 0.25: $\sigma = -0.2387P\,(X - Y)/d^2$, (1)

where σ represents the BFS (MPa), P represents the total load causing the fracture (N), and d represents the specimen disk thickness at the fracture origin (1 mm). X and Y were calculated as follows:

$$X = (1 + \nu)\ln(r_2/r_3)^2 + [(1 - \nu)/2]\,(r_2/r_3)^2 \qquad (2)$$

$$Y = (1 + \nu)[1 + \ln(r_1/r_3)^2] + (1 - \nu)(r_1/r_3)^2, \qquad (3)$$

where ν represents the Poisson's ratio, r_1 represents the radius of the support circle (6.0 mm), r_2 represents the radius of the loaded area (0.70 mm), and r_3 represents the radius of the specimen (6.5 mm).

The 3-point flexural strength of each specimen was calculated using the following equation obtained from ISO Standard 6872: $\sigma = 3PL/2wb^2$, where P represents the load at failure, l represents the outer span (20.0 mm), w represents the width of the bar (4.0 mm), and b represents the thickness of the bar (3.0 mm).

6. Silicone replica technique

The silicone replica technique was used to examine the marginal and internal gaps in the crowns. Twenty sets of crowns were filled with silicone registration material (Fit Checker Advanced, GC Corp.) and seated on the titanium die, which was held in place for 3 seconds with the maximum finger pressure to simulate the clinical cementation of the crown. After 1 minute, the impression material fully hardened. In all cases, the crown and titanium die were separated, with the silicone registration material still attached to the inner surface of the crown. To stabilize the silicone registration material adhered to the inner surface of the crown, another light-body polyvinyl siloxane (Exafine Light body, GC Corp.) was injected into the crown to form a one-piece without distortion. Once the silicone replica was completed, it was bisected mesiodistally. The buccal, lingual, mesial, and distal sides were measured. The four measurement points were the margin, axial wall, line angle, and occlusal plane. The marginal gap measured in this study is identical to that described by Holmes et al. (Holmes et al., 1989) as measured perpendicularly from the internal surface of the margin of the crown or casting to the outermost edge of the finish line of the tooth margin. Images were captured using a stereomicroscope (SMZ-168, Motic) at 8× magnification and analyzed using image analysis software (ImageJ, NIH) (Figure 4).

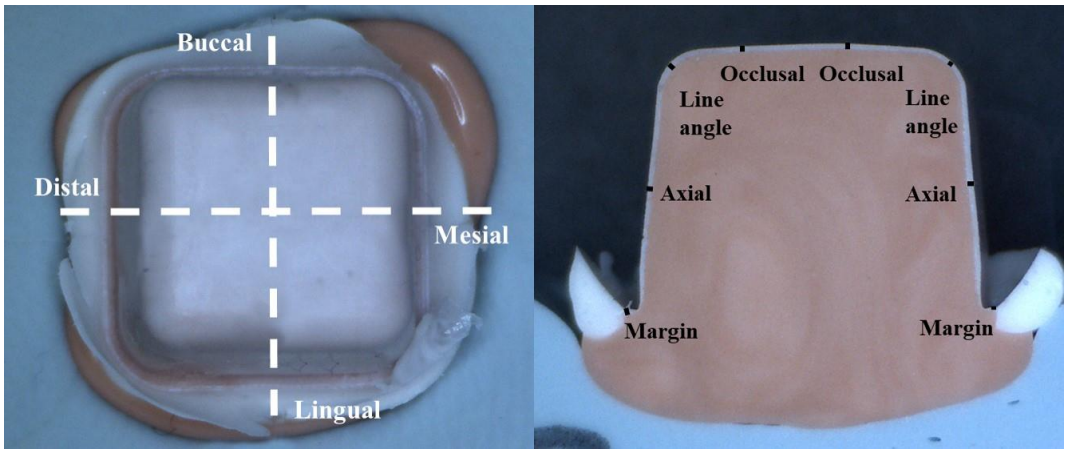

Figure 4. Crown specimen sections and measurement locations: (a) lines indicating specimen sections; (b) cross-sectional view of measurement locations.

7. Statistical analysis

Statistical software (SPSS statistics v27; IBM Corp., Armonk, NY, USA) was used for statistical analyses. The normality of all data values was evaluated using the Shapiro–Wilk test. A linear mixed model was used to determine the significance of the interaction effect between the CNC and AM groups; the increase in the monoclinic phase fraction and decrease in the biaxial bending strength over time were significant. At each time point, a Mann–Whitney U test (or independent t-test) was conducted to determine whether there was a difference between the CNC and AM groups. Pearson correlation analysis was performed for each group and time combination to confirm the correlation between the monoclinic phase fraction and BFS. The level of significance (p-value) was set at $p < 0.05$.

Similarly, an independent t-test was performed to determine whether there was a significant difference in the gaps between the CNC and AM groups. Non-inferiority trials were conducted to verify that whether the gaps in the zirconia crowns in the AM group were non-inferior to those in the CNC group. The two groups were compared to check for statistically significant differences in the gaps between the groups at 95% confidence intervals (CIs). To determine whether the AM group was non-inferior to the CNC group, non-inferiority cutoff points were derived by calculating 95% confidence intervals for the difference in the marginal and internal gaps between the CNC and placebo groups,

referencing Nayana Paul et al. (Paul et al., 2020). As a result, the non-inferior margin was set as −33. Repeat measurements using the one-way ANOVA statistical test were carried out ($p < 0.05$) to examine significant differences between the groups.

III. Results

1. Microstructural analysis

Figures 5 and 6 present SEM images of the zirconia ceramics before and after autoclaving for each group. The left side shows the microstructure before autoclaving, and the right side shows the microstructure after autoclaving for 5, 10, and 24 h. The SEM images indicate that the CNC group has a relatively amorphous crystal structure, whereas the AM group has a relatively angled crystal structure. Furthermore, the SEM images indicate the presence of pores in the AM specimens. As the autoclave time increased, both the CNC and AM specimens tended to aggregate.

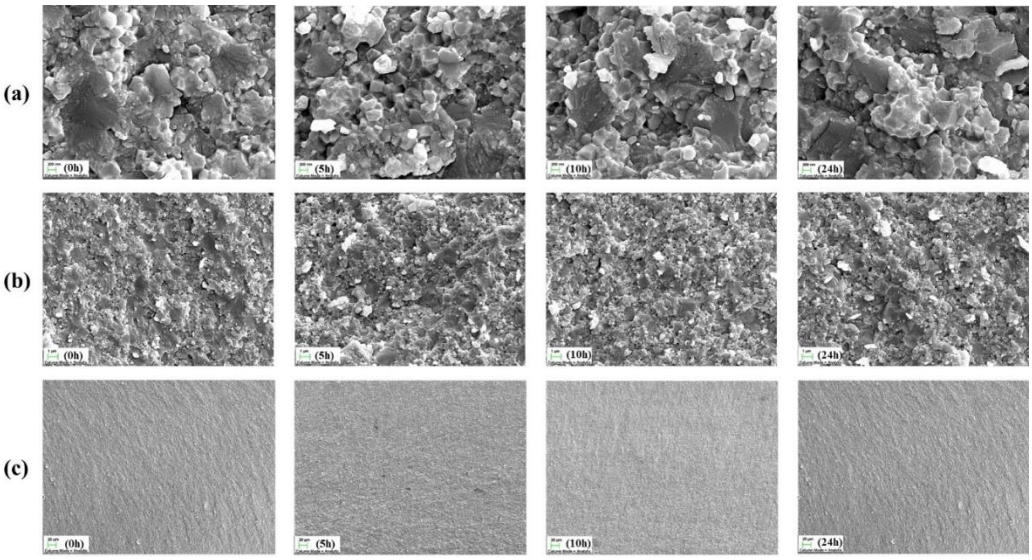

Figure 5. Cross-sectional SEM images of CNC specimens at different magnifications: (a) scale bar represents 200 nm; (b) scale bar represents 1 μm; (c) scale bar represents 20 μm.

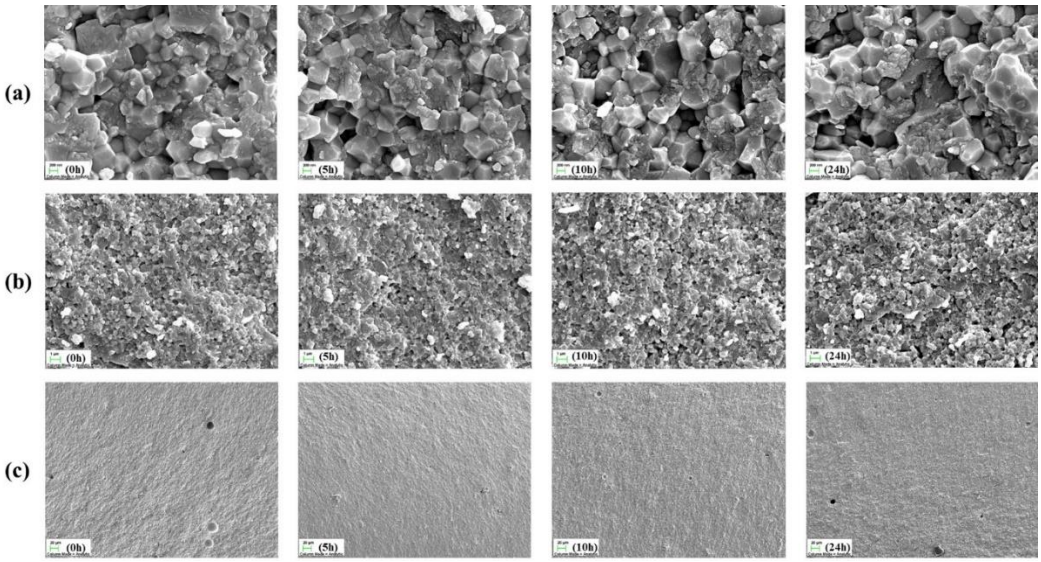

Figure 6. Cross-sectional SEM images of AM specimens at different magnifications: (a) scale bar represents 200 nm; (b) scale bar represents 1 μm; (c) scale bar represents 20 μm.

2. m-Phase fraction and flexural strength

Table 1 presents the mean and SD of the m-phase fraction (vol%) and flexural strength (MPa) of each group over time. Table 2 presents the results of the Shapiro–Wilk normality test for the m-phase fraction (vol%), biaxial flexural strength (MPa), and 3-point bending strength (MPa) for each group–time point combination. The normality test indicated that the biaxial flexural strength (MPa) and 3-point bending strength (MPa) were normal in each group ($p > 0.05$). However, the m-phase fraction (vol%) did not follow a normal distribution ($p < 0.05$) in the CNC group at 5 h ($p < 0.001$) or in the AM group at 24 h ($p < 0.001$).

Table 1. Experimental results for the monoclinic phase fraction, biaxial flexural strength test, and 3-point bending strength test; monoclinic phase fraction = m-phase (vol%), biaxial flexural strength = B, 3-point bending strength = T, results are presented as mean ± SD.

Group	m-phase (vol%)	B (MPa)	T (MPa)
CNC 0h	3.6638 ± 0.0002	1381.496 ± 321.620	1175.044 ± 117.655
CNC 5h	17.7198 ± 0.0002	1250.011 ± 282.534	
CNC 10h	26.0482 ± 0.0002	1230.006 ± 213.807	
CNC 24h	50.6824 ± 0.0003	1173.432 ± 207.294	
AM 0h	1.5307 ± 0.0003	1017.034 ± 209.643	743.6623 ± 64.726
AM 5h	13.3794 ± 0.0002	1011.763 ± 197.902	
AM 10h	43.0652 ± 0.0002	1034.681 ± 249.805	
AM 24h	76.3569 ± 0.0002	997.5798 ± 197.430	

Table 2. Normality test results of the Shapiro–Wilk test for each group–time point combination for the monoclinic phase fraction, biaxial flexural strength, and 3-point bending strength; monoclinic phase fraction = m-phase (vol%), biaxial flexural strength = B, 3-point bending strength = T.

Variable	**Shapiro–Wilk test**		
	W	Df	p-value
m-phase (vol%)			
0 h			
CNC	0.914	10	0.310
AM	0.971	10	0.903
5 h			
CNC	0.367	10	<0.001
AM	0.804	10	0.016
10 h			
CNC	0.936	10	0.513
AM	0.922	10	0.374
24 h			
CNC	0.933	10	0.476
AM	0.366	10	<0.001
B (MPa)			
0 h			
CNC	0.923	10	0.380

Variable	**Shapiro–Wilk test**		
	W	Df	p-value
AM	0.927	10	0.418
5 h			
CNC	0.889	10	0.164
AM	0.953	10	0.709
10 h			
CNC	0.959	10	0.772
AM	0.931	10	0.459
24 h			
CNC	0.930	10	0.443
AM	0.967	10	0.864
T (MPa)			
0 h			
CNC	0.850	10	0.058
AM	0.905	10	0.248

Linear mixed models were used to test the significance of the interaction effect between the CNC, AM, and autoclaving groups and the increase in the m-phase fraction and decrease in the BFS over time. The analysis of the m-phase fraction by group according to the autoclave time is presented in Table 3 and Figure 7. In Figure 7, the m-phase fraction for both the CNC and AM groups increases with the autoclave time. It increases more rapidly for the AM group than for the CNC group. Table 4 and Figure 8 present the analysis of the differences in biaxial flexural strength by group according to the autoclave time. In Figure 8, the biaxial flexural strengths of both groups decrease with an increase in the autoclave time; however, the reductions are gradual rather than sharp.

Table 3. Monoclinic phase fraction (vol%) according to the autoclave time for the CNC and AM groups.

	0 h	5 h	10 h	24 h	p for trend*	p for interaction**
CNC	3.66 ± 0.00	17.67 ± 0.17	26.05 ± 0.00	50.68 ± 0.00	<0.001	<0.001
AM	1.53 ± 0.00	13.38 ± 0.00	43.07 ± 0.00	76.06 ± 0.95	<0.001	
p for difference†	<0.001	<0.001	<0.001	<0.001		

Values are presented as mean ± SD.

* p for trend over time within each group in linear mixed model

** p for interaction between group and time in linear mixed model

† p for difference between two groups within each time point based on Mann–Whitney U test

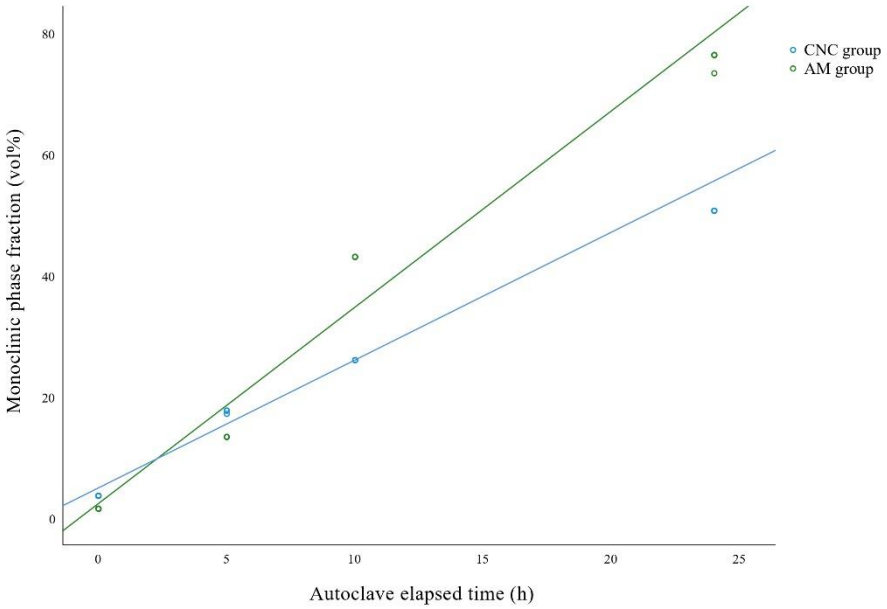

Figure 7. Scatter plot for the monoclinic phase fraction (vol%). The solid line is an estimate of the linear mixed linear model.

Table 4. Biaxial flexural strength (MPa) according to the autoclave time for the CNC and AM groups.

	0 h	5 h	10 h	24 h	p for trend*	p for interaction**
CNC	1381.50 ± 339.02	1250.01 ± 297.82	1230.01 ± 225.37	1173.43 ± 218.51	0.0502	0.282
AM	1017.03 ± 220.98	1011.76 ± 208.61	1034.68 ± 263.32	997.58 ± 208.11	0.547	
p for difference†	0.011	0.053	0.092	0.082		

Values are presented as mean ± SD.

* p for trend over time within each group in the linear mixed model

** p for interaction between group and time in linear mixed model

† p for difference between two groups within each time point based on independent t-test

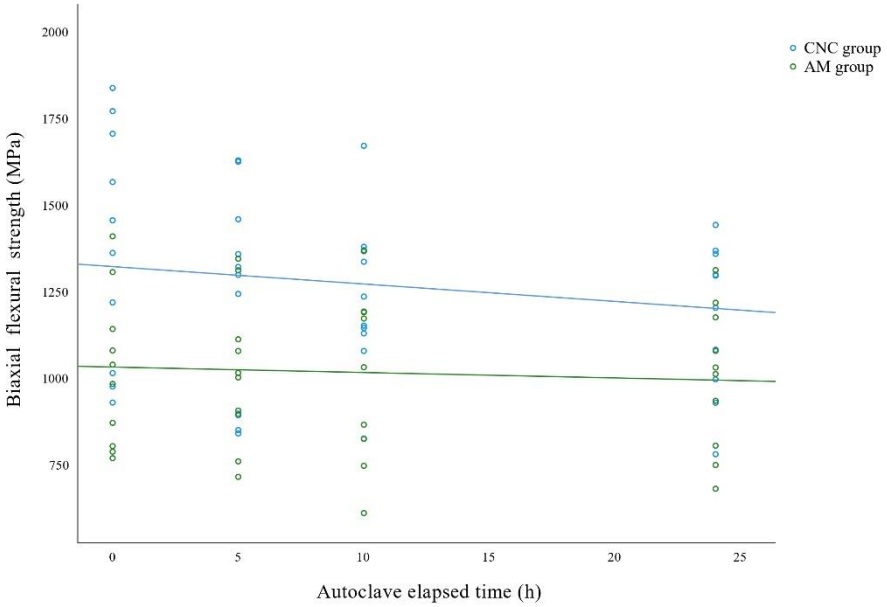

Figure 8. Scatter plot for biaxial flexural strength (MPa). The solid line is an estimate of the linear mixed linear model.

Pearson correlation analysis was performed for each group–time point combination to determine the correlation between the monoclinic phase fraction and the BFS, as shown in Table 5. The analysis revealed a p-value of < 0.05 at only two time points of autoclaving: 0 and 5 h. Thus, it can be concluded that there is a significant correlation between the m-phase fraction and BFS only at 0 and 5 h. In Figure 9, there is no overall correlation between the m-phase fraction and the biaxial flexural strength.

Table 5. Pearson's correlation analysis of the monoclinic phase fraction and biaxial flexural strength.

Objects	N	Coefficient	p-value
Totality	80	–0.184	0.102
By time			
0 h	20	0.557	0.011
5 h	20	0.457	0.043
10 h	20	–0.387	0.092
24 h	20	–0.407	0.075
By group			
CNC	40	–0.256	0.111
AM	40	–0.024	0.881
Group - Time Point Combination			
CNC			
0 h	10	–0.128	0.724
5 h	10	0.474	0.166
10 h	10	0.084	0.818
24 h	10	–0.222	0.538
AM			
0 h	10	–0.105	0.773
5 h	10	–0.411	0.238
10 h	10	0.097	0.790
24 h	10	–0.297	0.405

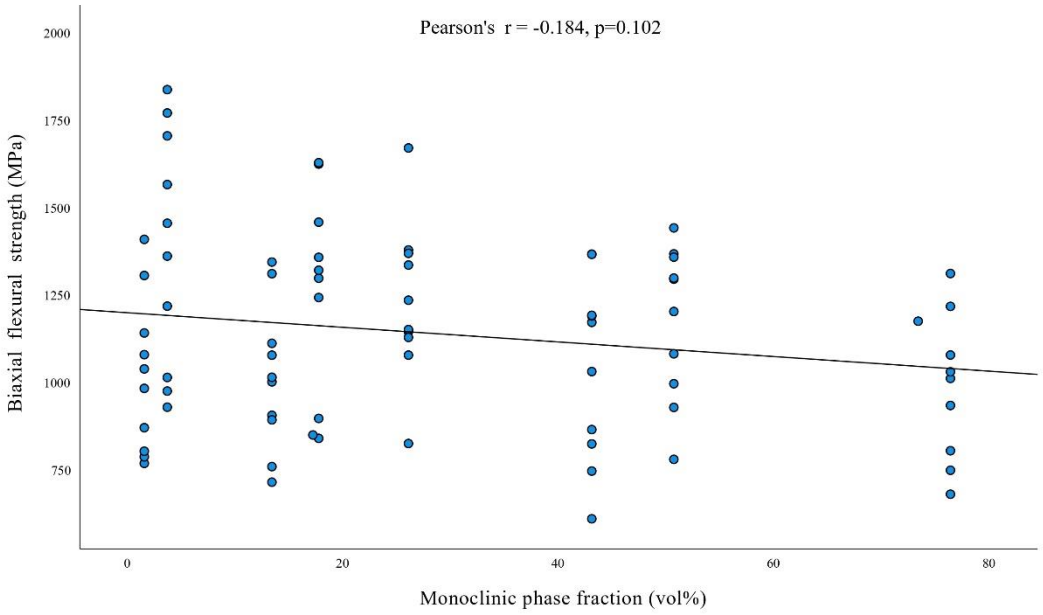

Figure 9. Scatter plot of the monoclinic phase fraction and biaxial flexural strength.

3. Marginal and internal gaps

The Shapiro–Wilk test was performed to determine whether the marginal and internal gaps of the CNC and AM groups satisfied normality. As shown in Table 6, only the marginal gap in the AM group did not satisfy normality. However, the QQ plot of the data indicates that the normality is a reasonable assumption.

Table 6. Shapiro–Wilk test normality test results for the marginal and internal gaps by group.

Shapiro–Wilk test		**Group**	W	Df	p-value
Marginal gap		CNC	0.982	40	0.753
		AM	0.864	40	<0.001
Internal gap	Axial	CNC	0.985	40	0.870
		AM	0.952	40	0.087
	Line angle	CNC	0.965	40	0.249
		AM	0.975	40	0.507
	Occlusal	CNC	0.977	40	0.574
		AM	0.953	40	0.097

The non-inferiority trials were conducted between the CNC and AM groups at each measurement point. The lower bound of the 95% CI of the difference value (CNC group gap – AM group gap) was compared with the non-inferiority coefficient of −33. The lower bound of all CIs was below −33, except for the distal part of the internal occlusal gap. Therefore, it cannot be concluded that the AM group gap was not inferior to the CNC group gap. In the internal occlusal gap, the lower limit of the CI was above −33 for the distal region, indicating that the gap in the AM group was not inferior to that in the CNC group (Table 7 and Figure 10).

Table 7. Site-specific differences between the CNC and AM groups.

Location			Group	Mean	SD	Difference	95% CI of difference	
							Lower	Upper
Marginal gap		B	CNC	38.00	11.78	–17.50	–43.43	8.43
			AM	55.50	37.21			
		L	CNC	56.10	15.29	–49.90	–88.85	–10.95
			AM	106.00	53.46			
		M	CNC	42.50	16.13	–51.70	–107.87	4.47
			AM	94.20	77.81			
		D	CNC	53.30	16.78	–20.80	–41.94	0.34
			AM	74.10	27.03			
Internal gap	Axial	B	CNC	103.20	24.09	–10.30	–51.97	31.37
			AM	113.50	55.62			
		L	CNC	95.40	11.95	–54.30	–85.55	–23.05
			AM	149.70	42.94			
		M	CNC	101.40	25.94	–9.90	–43.83	24.03
			AM	111.30	44.00			
		D	CNC	121.50	20.96	–32.90	–70.32	4.52
			AM	154.40	52.28			
	Line angle	B	CNC	104.60	44.01	–66.40	–107.98	–24.82
			AM	171.00	44.49			
		L	CNC	105.70	38.43	–114.40	–	–77.20

			AM	220.10	40.73		151.60	
		M	CNC	88.90	29.10	–62.60	–97.19	–28.01
			AM	151.50	43.16			
		D	CNC	143.70	39.53	–86.20	–126.65	–45.75
			AM	229.90	46.32			
	Occlusal	B	CNC	187.30	14.11	–37.20	–56.17	–18.23
			AM	224.50	24.83			
		L	CNC	184.00	12.11	–43.10	–67.53	–18.67
			AM	227.10	33.09			
		M	CNC	187.40	11.50	-49.90	–71.62	–28.18
			AM	237.30	29.26			
		D	CNC	192.10	18.32	–17.80	–36.32	0.72
			AM	209.90	21.01			

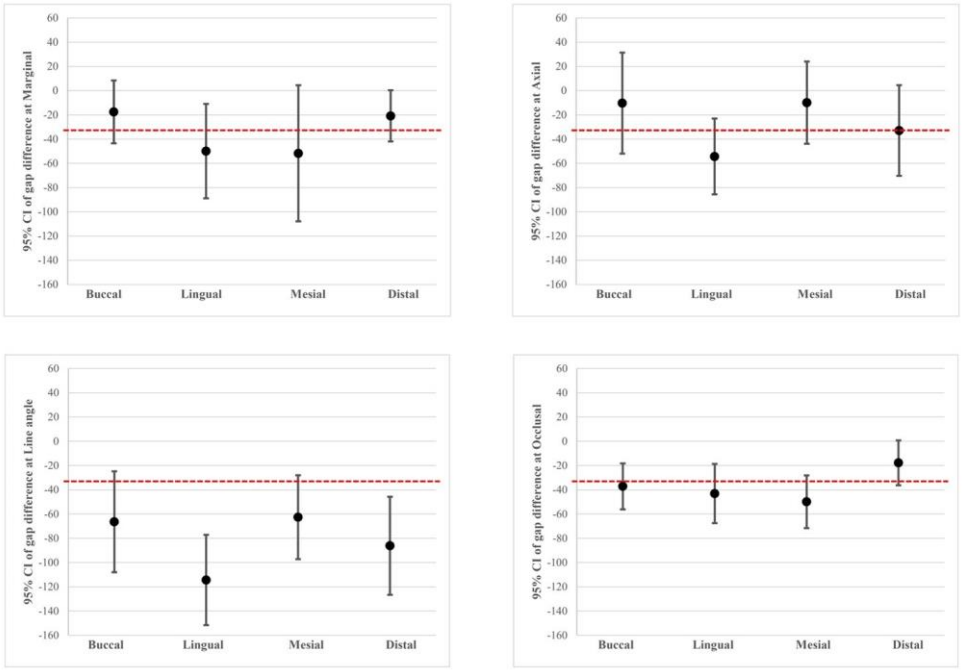

Figure 10. Two-sided 95% CI for the gap difference between the CNC and AM groups at various locations.

Figure 11,12,13,14 show the mean values with standard errors for the margin, axial wall, line angle and occlusal plane gaps as measured in 4 locations (buccal, lingual, mesial, and distal) for crowns fabricated by the CNC and AM technologies. The marginal and internal gap values of AM group were lager than CNC group crowns.

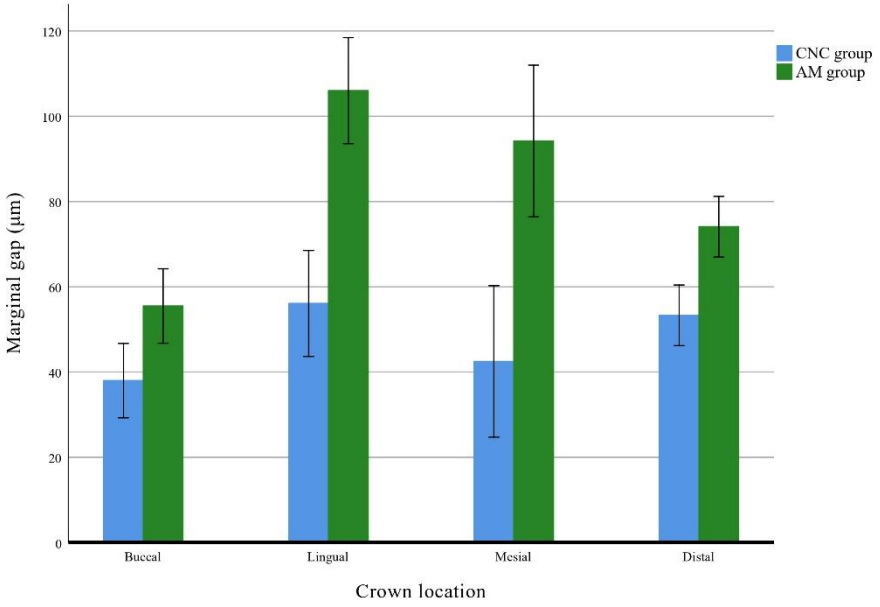

Figure 11. Comparison of mean values and standard errors of marginal gap at different locations for CNC and AM group crowns.

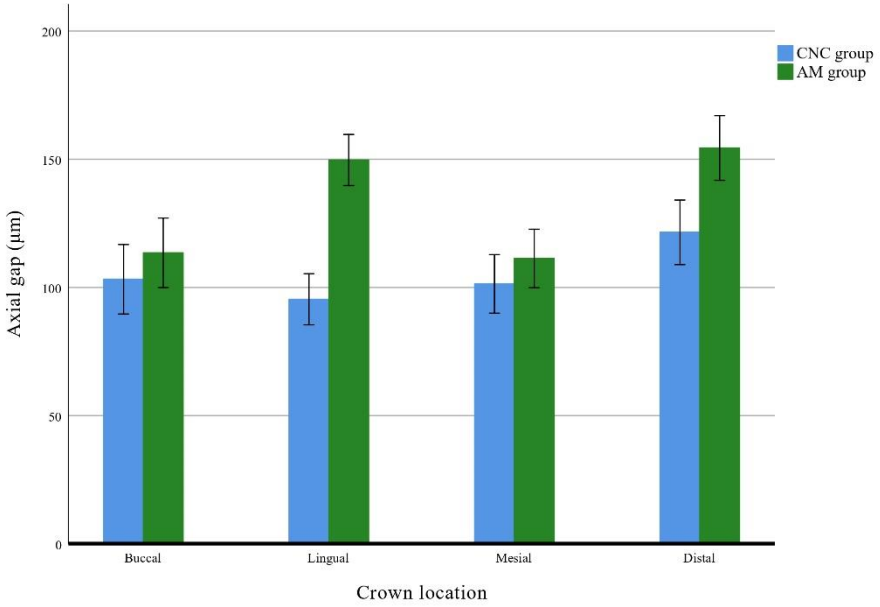

Figure 12. Comparison of mean values and standard errors of axial gap at different locations for CNC and AM group crowns.

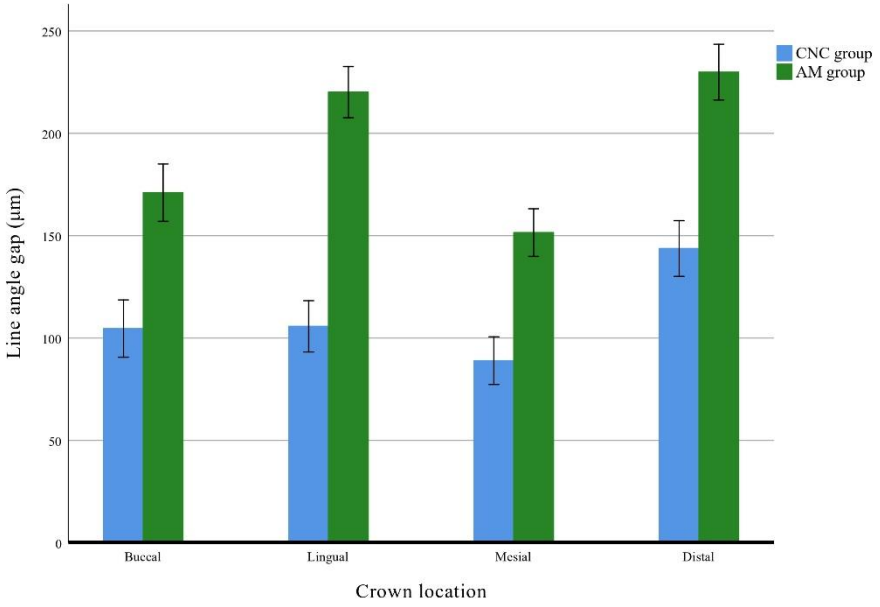

Figure 13. Comparison of mean values and standard errors of line angle gap at different locations for CNC and AM group crowns.

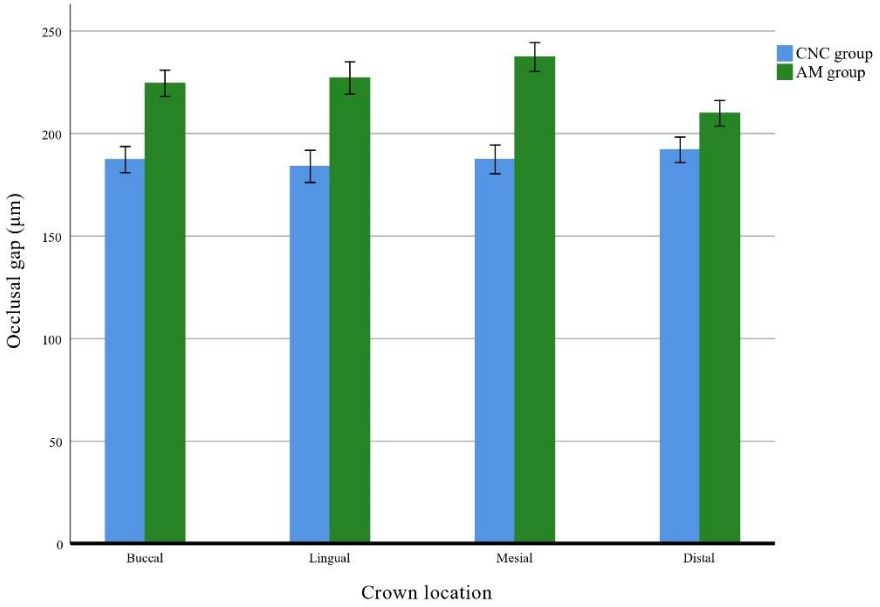

Figure 14. Comparison of mean values and standard errors of occlusal gap at different locations for CNC and AM group crowns.

The overall mean ± standard error (SE) value for marginal and internal (axial, line angle and occlusal) gaps of the CNC and AM group crowns are presented in Table 8. The statistical outcome showed significant differences for all groups.

Table 8. Least squares mean and standard error of marginal and internal gaps.

			CNC group	AM group	p*
			LS mean ± SE		
Marginal gap		Total	47.48 ± 6.98	82.45 ± 6.98	0.002
		B	38.00 ± 8.73	55.50 ± 8.73	
		L	56.10 ± 12.43	106.00 ± 12.43	
		M	42.50 ± 17.77	94.20 ± 17.77	
		D	53.30 ± 7.11	74.10 ± 7.11	
Internal gap	Axial	Total	105.38 ± 3.02	132.23 ± 3.02	<0.001
		B	103.20 ± 13.55	113.50 ± 13.55	
		L	95.40 ± 9.97	149.70 ± 9.97	
		M	101.40 ± 11.42	111.30 ± 11.42	
		D	121.50 ± 12.60	154.40 ± 12.60	
	Line angle	Total	110.73 ± 8.52	193.13 ± 8.52	<0.001
		B	104.60 ± 13.99	171.00 ± 13.99	
		L	105.70 ± 12.52	220.10 ± 12.52	
		M	88.90 ± 11.64	151.50 ± 11.64	
		D	143.70 ± 13.62	229.90 ± 13.62	
	Occlusal	Total	187.70 ± 4.95	224.70 ± 4.95	<0.001

		B	187.30 ± 6.39	224.50 ± 6.39	
		L	184.00 ± 7.88	227.10 ± 7.88	
		M	187.40 ± 7.03	237.30 ± 7.03	
		D	192.10 ± 6.23	209.90 ± 6.23	

Values were presented by Least squares means ± standard errors in repeated measures one-way ANOVA.

* P for difference between two groups in repeated measures one-way ANOVA

IV. Discussion

We evaluated the mechanical properties of zirconia restorations fabricated via subtractive machining and additive manufacturing. In addition, the accuracy of the crowns was evaluated. The null hypothesis, which states that the mechanical properties of 3Y-TZP restorations fabricated using AM technology are comparable to those of 3Y-TZP restorations fabricated using CNC technology, is accepted. This study rejects the null hypothesis that the marginal and internal gaps of 3Y-TZP crowns fabricated using AM technology are similar to those of 3Y-TZP crowns fabricated using CNC technology. Significant differences were observed between the subtractive and additive processes at all the sites. For the instrumented section (buccal, lingual, mesial, distal), the null hypothesis of non-inferiority was rejected, as the results indicated inferiority at all sites (lower limit CI < -33), except for the distal site in the occlusal section ($p < 0.05$). The repeated-measures one-way ANOVA revealed that the marginal and internal gaps of AM-produced zirconia crowns were less accurate than those of CNC-produced zirconia crowns ($p < 0.05$).

Figures 5 and 6 present SEM images of the zirconia ceramics for each group with respect to the autoclave time. The crystal grains of the AM group were more angular than those of the CNC group. Figure 6(c) shows pores for the AM group, which is characteristic of additively manufactured zirconia (Ebert et al., 2009). This is attributed to the differences in the processes used to prepare the zirconia blocks or slurries and the processing methods

used. Zirconia powder and binders are the basic ingredients used to prepare zirconia blocks and slurries. The zirconia blocks are created by feeding them into a hot press and applying pressure and temperature to solidify them. This process causes the zirconia powder to adhere and debind to some extent, and the debinding is completed through post-processing sintering. In the AM method, a zirconia slurry is prepared by adding a fine powder to a hydrophilic or hydrophobic light-curable polymeric medium (Griffith et al., 1996; Chen et al. 2010). An even distribution of fine ceramic particles in a polymeric medium is crucial for the curing reaction to occur under irradiation. This has been achieved using surfactants and other additives. An unstable suspension can cause rapid separation of the ceramic polymer, leading to material inhomogeneity in the final product (Komissarenko et al., 2018). The prefabricated ceramic–polymer composite shapes undergo a post-treatment sintering process to remove all organic matter. The zirconia specimens used in this study were post-processed. From a comparison of the CNC group at 0 h (Figure 5(c), 0 h) and AM group at 0 h (Figure 6(c), 0 h), it is believed that the pores observed in the AM group specimens resulted from the uneven dispersion of ceramic particles in the zirconia slurry in the AM processing method. Herrer et al. showed that porosity problems in AM-produced specimens may arise from the large volume fraction of the binder in the green bodies (Harrer et al., 2017). If binder burnout is insufficient and/or the sintering process is not optimized, large pores may exist in the sintered body.

The XRD results indicated that the m-phase fraction increased in both the CNC

and AM groups when the zirconia specimens were aged for 5, 10, and 24 h. The CNC group exhibited increases from 17.67 ± 0.17 vol% at 5 h to 26.05 ± 0.00 vol% at 10 h and 50.68 ± 0.00 vol% at 24 h. The AM group exhibited increases from 13.38 ± 0.00 vol% at 5 h to 43.07 ± 0.00 vol% at 10 h and 76.06 ± 0.95 vol% at 24 h. According to ISO 13356, the m-phase fraction of zirconia in ceramic materials based on Y-TZP for implant surgery should not exceed 25% after aging for 5 h at 134 °C and 0.2 MPa. The m-phase fraction for the CNC group after aging for 5 h was 17.67 ± 0.17 vol%, and that for the AM group was 13.38 ± 0.00 vol%, both of which meet this standard. However, the aging for the AM group was rapid, and the m-phase content reached 43.07 ± 0.00 vol% after 10 h of aging and exceeded 76.06 ± 0.00 vol% after 24 h. In comparison, the m-phase fraction of the CNC group increased relatively slowly, indicating a better aging resistance.

The flexural strength test is the most commonly used method for testing dental ceramics owing to its relatively simple specimen preparation procedure. There are two methods for conducting flexural strength tests: biaxial flexural strength (BFS) tests and 3-/4-point bending strength tests. However, the 3-/4-point flexure tests have a significant drawback: it is difficult to eliminate unwanted edge failures. Therefore, BFS tests are frequently conducted to determine the fracture characteristics of ceramic materials (Ban and Anusavice, 1990; Ritter et al., 1980). However, it has not yet been clearly confirmed whether there are relationships between the flexural strengths of dental ceramics using these tests. Several studies have focused on the relationship between the BFS test and the

3-point bending strength test for dental ceramics. Although differences exist among manufacturers, in most cases, the BFSs of dental ceramics significantly exceed the 3-point bending strengths (Jin et al., 2004; Wendler et al., 2017). Furthermore, in several studies comparing flexural strength tests of zirconia ceramics, 3-/4-point flexural strengths were lower than BFSs (Schatz et al., 2016). In the present study, the CNC and AM groups exhibited normal distributions for both the BFS and 3-point bending strength tests (Table 2). As previously reported, for both groups (CNC 0 h: 1381.496 ± 321.620 MPa, AM 0 h: 1017.034 ± 209.643 MPa), the BFS exceeded the 3-point bending strength (CNC 0 h: 1175.044 ± 117.655 MPa, AM 0 h: 743.6623 ± 64.726 MPa). Therefore, the BFS test was selected to evaluate the flexural strength of the disk specimens after the LTD experiment. In Abuslsaud et al.'s study (Abualsaud et al., 2022), the flexural strength of AM-produced zirconia (milled disc-shaped specimens: 1507.27 ± 340.10 MPa, 3D-printed disc-shaped specimens in horizontal orientation: 1186.76 ± 283.47 MPa) was comparable to that of CNC-produced zirconia.

The BFS results indicated that for both the CNC and AM groups, the flexural strengths of the zirconia specimens were reduced after aging for 5, 10, and 24 h. The flexural strength of the CNC group decreased from 1250.01 ± 297.82 MPa to 1173.43 ± 218.51 MPa, and that of the AM group decreased from 1011.76 ± 208.61 MPa to 997.58 ± 208.11 MPa. However, the BFS of the specimens did not decrease significantly as the aging time increased for either the CNC or AM group, as indicated by the gradually decreasing

slopes in Figure 8. In ISO 6872, dental ceramics are classified into five classes based on their intended clinical use. In addition, the mean flexural strength values for both groups met the criteria for class 5 (800 MPa) in ISO 6872. According to the class 5 criteria, the recommended clinical indication is monolithic ceramics for the substructure of partial or full coverage prostheses of 4 units or more.

LTD involves the phase transition of zirconia from the tetragonal to the monoclinic phase. The strength of zirconia decreases rapidly when this occurs. Analysis of the differences in the m-phase fraction and BFS over time between the groups revealed an increase in the monoclinic phase fraction and a decrease in the flexural strength over time, similar to the results of previous studies (Zhai et al., 2021).

The Pearson correlation analysis conducted to examine the correlation between the m-phase fraction and the BFS in this study revealed a significant correlation only at two time points: 0 h ($p = 0.011$) and 5 h ($p = 0.043$), as shown in Table 5. However, there appears to be no significant correlation between the m-phase content and the BFS, as shown in Figure 9.

Currently, there is no consensus regarding the maximum marginal gap for clinically accepted dental restorations. However, numerous researchers have reported that marginal gaps ranging from 50 to 300 μm are clinically acceptable (McLean et al., 1971; Hung et al., 1990; Moldovan et al., 2006; Quante et al., 2008; Ucar et al., 2009). In a systematic review, the marginal gap was reported to be 7.6–206.3 μm for ceramic crowns

(Contrepois et al., 2013). Studies related to the fit of CAD-CAM restorations have reported marginal gaps of 39–201 μm and internal gaps of 23–230 μm. These measurements indicate a clinically acceptable marginal fit, as the commonly used criteria for evaluating fit are <120 μm. In the present study, the marginal gap of zirconia crowns fabricated via CNC and AM was <120 μm; it was 47.48 ± 16.37 μm for the CNC group and 82.45 ± 54.10 μm for the AM group. However, regarding the medial gap, the occlusal gap in the CNC group (187.70 ± 14.01 μm) and the axial wall (132.23 ± 51.22 μm), line angle (193.13 ± 53.55 μm), and occlusal gap (224.70 ± 28.16 μm) in the AM group exceeded the evaluation range of 120 μm. Nonetheless, they were all within the broad clinical acceptance range of 300 μm; thus, they can be considered clinically acceptable. We found that CNC-produced zirconia crowns provided a tighter fit than AM crowns, as both the marginal and internal gaps in the AM group were significantly larger than those in the CNC group. These results are consistent with the findings of Revilla-Leon et al., who reported that CNC-produced zirconia crowns had tighter marginal and internal gaps than AM-produced crowns, and both methods provided a clinically acceptable fit (Revilla et al., 2020). However, Li et al. reported that the internal and marginal adaptations of stereolithography-produced zirconia crowns were not suitable for clinical applications (Li et al., 2019). A non-inferiority test was conducted on instrumented sections (buccal, lingual, mesial, and distal), and it was found that the gap of AM-produced zirconia crowns was inferior to that of CNC-produced zirconia crowns in all sections except for the distal section of the occlusal section (lower

limit CI < −33). Therefore, it cannot be concluded that the AM group gap was not inferior to the CNC group gap. In addition to the repeated-measures one-way ANOVA revealed that the marginal and internal gaps of AM-produced zirconia crowns were less accurate than those of CNC-produced zirconia crowns ($p < 0.05$). This indicates that the gap in AM-produced zirconia crowns is within the clinically acceptable range but is inferior to that of CNC-produced zirconia crowns. This outcome prompts the consideration of volumetricization in the field of manufacturing. Similarly to subtractive manufacturing, additive manufacturing necessitates the sintering process subsequent to printing. Moreover, this process necessitates the removal of photosensitive resin. In subtractive manufacturing, the shrinkage of approximately 20 to 30 percent of the total volume that accompanies the sintering process is compensated for by the expanded digital design of the restoration (Manicone et al., 2007). However, the extent of sintering shrinkage in the additive manufacturing process remains uncertain, making it challenging to determine the extent to which digital design compensation is necessary. This is reflected in the larger gap observed in the crowns produced by the additive manufacturing process relative to those produced by subtractive manufacturing, as demonstrated in this study. Consequently, it is anticipated that once the volumization issue is addressed, crown accuracy will be comparable to that achieved through subtractive manufacturing.

The results of this limited study demonstrate that the mechanical properties of additively manufactured zirconia meet the requirements for clinical applications. Studies

that compare the mechanical and physical performances of 3D-printed zirconia with those of CNC-milled restorations are limited because 3D-printing of ceramic dental restorations is in the early stages of development. In addition, the fit, precision, and accuracy of full-contour 3D-printed monolithic zirconia crowns have not been extensively investigated. In this study, specimens that had completed the printing and finishing processes were analyzed. Therefore, the results obtained herein do not account for the critical manufacturing issues that affect the material performance. Hence, it is necessary to investigate in detail the nature of the raw materials used in the additive technology and their concentrations (which determine the rheological properties of the suspension), parameters (e.g., printing speed, layer height/line width, orientation, nozzle/light source characteristics), post-printing treatments (e.g., debinding and sintering) and surface finishing (Branco et al., 2023).

V. Conclusion

Within the limitations of this study, the following conclusions are drawn:

The mechanical properties of AM-produced 3Y-TZP are comparable to those of CNC-produced 3Y-TZP restorations, and the marginal and internal gaps of AM-produced 3Y-TZP are not comparable to those of CNC-produced 3Y-TZP crowns; however, in both cases, they are within the clinically acceptable range.

Acknowledgments

This work was supported by the Technology Innovation Program (Development of material parts technology) (20001155, Development of Highly Transluscent Tough Ceramic Materials and Manufacturing Technique for Tailormade Crown) funded By the Ministry of Trade, Industry & Energy(MOTIE, Korea)

VI. References

Abualsaud, R., Abussaud, M., Assudmi, Y., Aljoaib, G., Khaled, A., Alalawi, H., Akhtar, S., Matin, A., & Gad, M. M. (2022). Physiomechanical and Surface Characteristics of 3D-Printed Zirconia: An In Vitro Study. *Materials (Basel, Switzerland),* 15(19), 6988..

Alghazzawi T. F. (2016). Advancements in CAD/CAM technology: Options for practical implementation. *Journal of prosthodontic research,* 60(2), 72–84.

Ban, S., & Anusavice, K. J. (1990). Influence of test method on failure stress of brittle dental materials. *Journal of dental research,* 69(12), 1791–1799.

Chen, Z., Li, D., Zhou, W., & Wang, L. (2010). Curing characteristics of ceramic stereolithography for an aqueous-based silica suspension. *Proceedings of the Institution of Mechanical Engineers, Part B: Journal of Engineering Manufacture,* 224(4), 641-651.

Christel, P., Meunier, A., Heller, M., Torre, J. P., & Peille, C. N. (1989). Mechanical properties and short-term in-vivo evaluation of yttrium-oxide-partially-stabilized zirconia. *Journal of biomedical materials research,* 23(1), 45–61.

Contrepois, M., Soenen, A., Bartala, M., & Laviole, O. (2013). Marginal adaptation of ceramic crowns: a systematic review. *The Journal of prosthetic dentistry,* 110(6), 447–454.e10.

Dawood, A., Marti Marti, B., Sauret-Jackson, V., & Darwood, A. (2015). 3D printing in

dentistry. *British dental journal*, 219(11), 521–529.

Deckers, J., Vleugels, J., & Kruth, J. P. (2014). Additive manufacturing of ceramics: A review. *Journal of Ceramic Science and Technology*, 5(4), 245-260.

Della Bona, A., Cantelli, V., Britto, V. T., Collares, K. F., & Stansbury, J. W. (2021). 3D printing restorative materials using a stereolithographic technique: a systematic review. *Dental materials : official publication of the Academy of Dental Materials*, 37(2), 336–350.

Denry, I., & Kelly, J. R. (2008). State of the art of zirconia for dental applications. *Dental materials : official publication of the Academy of Dental Materials*, 24(3), 299–307.

Ebert, J., Ozkol, E., Zeichner, A., Uibel, K., Weiss, O., Koops, U., Telle, R., & Fischer, H. (2009). Direct inkjet printing of dental prostheses made of zirconia. *Journal of dental research*, 88(7), 673–676.

Garvie, R. C., Hannink, R. H., & Pascoe, R. T. (1990). Ceramic steel?. In *Sintering Key* Papers (pp. 253-257). Dordrecht: Springer Netherlands.

Griffith, M. L., & Halloran, J. W. (1996). Freeform fabrication of ceramics via stereolithography. *Journal of the American Ceramic Society*, 79(10), 2601-2608.

Harrer, W., Schwentenwein, M., Lube, T., & Danzer, R. (2017). Fractography of zirconia-specimens made using additive manufacturing (LCM) technology. *Journal of the European Ceramic Society*, 37(14), 4331-4338.

Holmes, J. R., Bayne, S. C., Holland, G. A., & Sulik, W. D. (1989). Considerations in measurement of marginal fit. *The Journal of prosthetic dentistry*, *62*(4), 405–408.

Hung, S. H., Hung, K. S., Eick, J. D., & Chappell, R. P. (1990). Marginal fit of porcelain-fused-to-metal and two types of ceramic crown. *The Journal of prosthetic dentistry*, 63(1), 26–31.

Jin, J., Takahashi, H., & Iwasaki, N. (2004). Effect of test method on flexural strength of recent dental ceramics. *Dental materials journal*, 23(4), 490–496.

Kelly, J. R., & Denry, I. (2008). Stabilized zirconia as a structural ceramic: an overview. *Dental materials : official publication of the Academy of Dental Materials*, 24(3), 289–298.

Komissarenko, D. A., Sokolov, P. S., Evstigneeva, A. D., Shmeleva, I. A., & Dosovitsky, A. E. (2018). Rheological and Curing Behavior of Acrylate-Based Suspensions for the DLP 3D Printing of Complex Zirconia Parts. *Materials (Basel, Switzerland)*, 11(12), 2350..

Leinfelder, K. F., Isenberg, B. P., & Essig, M. E. (1989). A new method for generating ceramic restorations: a CAD-CAM system. *The Journal of the American Dental Association*, 118(6), 703-707.

Li, R., Wang, Y., Hu, M., Wang, Y., Xv, Y., Liu, Y., & Sun, Y. (2019). Strength and Adaptation of Stereolithography-Fabricated Zirconia Dental Crowns: An In Vitro Study. *The International journal of prosthodontics*, 32(5), 439–443.

Manicone, P. F., Rossi Iommetti, P., & Raffaelli, L. (2007). An overview of zirconia ceramics: basic properties and clinical applications. *Journal of dentistry*, *35*(11), 819–826.

McLean, J. W., & von Fraunhofer, J. A. (1971). The estimation of cement film thickness by an in vivo technique. *British dental journal*, 131(3), 107–111.

Moldovan, O., Rudolph, H., Quaas, S., Bornemann, G., & Luthardt, R. G. (2006). Internal and external fit of CAM-made zirconia bridge frameworks-a pilotstudy. *Deutsche Zahnarztliche Zeitschrift*, 61(1), 38.

Paul, N., Raghavendra Swamy, K. N., Dhakshaini, M. R., Sowmya, S., & Ravi, M. B. (2020). Marginal and internal fit evaluation of conventional metal-ceramic versus zirconia CAD/CAM crowns. *Journal of clinical and experimental dentistry*, *12*(1), e31–e37.

Quante, K., Ludwig, K., & Kern, M. (2008). Marginal and internal fit of metal-ceramic crowns fabricated with a new laser melting technology. *Dental materials : official publication of the Academy of Dental Materials*, 24(10), 1311–1315.

Rekow D. (1987). Computer-aided design and manufacturing in dentistry: a review of the state of the art. *The Journal of prosthetic dentistry*, 58(4), 512–516.

Rekow E. D. (1991). Dental CAD-CAM systems. What is the state of the art?. *Journal of the American Dental Association (1939),* 122(12), 42–48.

Ritter Jr, J. E., Jakus, K., Batakis, A., & Bandyopadhyay, N. (1980). Appraisal of biaxial

strength testing. *Journal of Non-Crystalline Solids*, 38, 419-424.

Revilla-León, M., Methani, M. M., Morton, D., & Zandinejad, A. (2020). Internal and marginal discrepancies associated with stereolithography (SLA) additively manufactured zirconia crowns. *The Journal of prosthetic dentistry*, 124(6), 730–737.

Stansbury, J. W., & Idacavage, M. J. (2016). 3D printing with polymers: Challenges among expanding options and opportunities. *Dental materials : official publication of the Academy of Dental Materials*, 32(1), 54–64..

Schatz, C., Strickstrock, M., Roos, M., Edelhoff, D., Eichberger, M., Zylla, I. M., & Stawarczyk, B. (2016). Influence of Specimen Preparation and Test Methods on the Flexural Strength Results of Monolithic Zirconia Materials. *Materials (Basel, Switzerland)*, 9(3), 180.

Torabi, K., Farjood, E., & Hamedani, S. (2015). Rapid Prototyping Technologies and their Applications in Prosthodontics, a Review of Literature. *Journal of dentistry (Shiraz, Iran)*, 16(1), 1–9.

Taormina, G., Sciancalepore, C., Messori, M., & Bondioli, F. (2018). 3D printing processes for photocurable polymeric materials: technologies, materials, and future trends. *Journal of applied biomaterials & functional materials*, 16(3), 151–160.

Ucar, Y., Akova, T., Akyil, M. S., & Brantley, W. A. (2009). Internal fit evaluation of crowns prepared using a new dental crown fabrication technique: laser-sintered

Co-Cr crowns. *The Journal of prosthetic dentistry*, 102(4), 253–259.

van der Zel J. M. (1993). Ceramic-fused-to-metal restorations with a new CAD/CAM system. *Quintessence international (Berlin, Germany : 1985)*, 24(11), 769–778.

Willmann, G., Früh, H. J., & Pfaff, H. G. (1996). Wear characteristics of sliding pairs of zirconia (Y-TZP) for hip endoprostheses. *Biomaterials*, 17(22), 2157–2162.

Wendler, M., Belli, R., Petschelt, A., Mevec, D., Harrer, W., Lube, T., Danzer, R., & Lohbauer, U. (2017). Chairside CAD/CAM materials. Part 2: Flexural strength testing. *Dental materials : official publication of the Academy of Dental Materials*, 33(1), 99–109.

Zhai, Z., & Sun, J. (2023). Research on the low-temperature degradation of dental zirconia ceramics fabricated by stereolithography. *The Journal of prosthetic dentistry*, 130(4), 629–638.

ABSTRACT (KOREAN)

적층 가공 방식으로 제작된 지르코니아 수복물의 기계적 특성 및 크라운의 정확도 평가

연세대학교 대학원 치의학과

<지도교수 **박 영 범**>

오 세 은

치과영역에서의 지르코니아는 우수한 물리적 특성과 생체적합성 및 적절한 광학적 성질을 가진 재료로 최근 CAD/CAM 기술의 발전과 함께 수복 재료로서 그 응용 범위가 넓어지고 있다. 최근 3D 프린팅 기술의 발전과 더불어 적층 가공 방식으로 지르코니아 세라믹 수복물을 제작하려는 시도가 있다. 따라서 본 연구는 적층 가공 방식으로 제작된 지르코니아 수복물의 기계적 특성과 지르코니아 크라운의 정확도를 비교하여 임상적 적용 가능성을 평가하고자 하였다.

절삭 가공 방식 (CNC group)과 적층 가공 방식 (AM group)으로 지르코니아 시편을 각 그룹 당 원판형 40 개, 막대형 10 개, 그리고 10 개의 크라운을 제작하였다. 이축 굴곡 강도와 3 점 굴곡 강도 측정을 위해 막대형 시편이 사용되었고, 각 그룹의 원판형 시편을 134℃, 215kPa 에서 5, 10, 24 시간 동안 열순환 처리를 시행하였으며, X-선 회절 분석을 통해 단사정상 분율과 이축 굴곡 강도 분석 후 통계 분석을 시행하였다. 제작된 크라운의 변연 및 내면 간격을 평가하기 위해 레플리카 기법이 사용되었다. 협설 및 근원심 단면의 변연, 축벽, 선각, 교합에서의 간격을 측정한 후 통계 분석을 시행하였다.

열순환 처리를 하지 않은 이축 굴곡 강도와 3 점 굴곡 강도는 두 그룹 모두에서 유의한 차이가 없었다 ($p > 0.05$). 열순환 처리를 시행한 각 그룹에서 단사정상 분율과 이축 굴곡 강도 간의 상관관계를 분석한 결과, 두 그룹 모두 열순환 처리 시간이 증가함에 따라 이축 굴곡 강도는 감소한 반면, 단사정상 분율은 증가한 것으로 나타났다. 하지만 두 그룹 모두 단사정상 분율과 이축 굴곡 강도 사이에 통계학적으로 유의한 상관관계는 없는 것으로 나타났다. 제작된 크라운의 두 그룹 간 변연 및 내면 간격을 비교한 Shapiro-Wilk test 결과 AM group 의 변연 간격에서만 유의한 차이가 있었지만, 전반적인 분포를 보았을 때 모든 계측점에서 두 그룹 사이에 유의한 차이가

없는 것으로 간주할 수 있었다. 계측 단면 별 (협측, 설측, 근심 및 원심)로 시행한 비열등성 시험 결과 AM group 의 교합 (원심) 부위를 제외한 (lower limit confidence interval > −33) 모든 계측 단면에서 CNC group 에 비해 열등하였다. 또한 계측 단면 별 (협측, 설측, 근심 및 원심)로 시행한 일원 반복 측정 분산 분석에서 AM group 의 모든 계측 단면에서 CNC group 에 대해 유의한 차이가 있었다 ($p < 0.05$).

이 연구의 한계 내에서, 적층 가공 방식으로 제작된 지르코니아 수복물은 절삭 가공 방식으로 제작된 것과 유사한 기계적 특성을 가지고, 크라운의 정확도는 절삭 가공 방식으로 제작된 것보다 열등하지만, 그 차이가 임상적으로 허용되는 범위에 속하므로, 임상적 적용이 가능할 수 있다는 것을 시사한다.

핵심되는 말: 3D 프린팅 지르코니아; 적층 가공 방식; 이축 굴곡 강도; 저온열화; 레플리카 기법